NMR study on dynamics of water molecules in concentrated aqueous zinc(II) bromide solutions at various temperatures

4 AUTHORS, INCLUDING:

Toshiyuki Takamuku
Saga University
84 PUBLICATIONS   **1,922** CITATIONS

SEE PROFILE

Toshio Yamaguchi
Fukuoka University
203 PUBLICATIONS   **3,783** CITATIONS

SEE PROFILE

Hisanobu Wakita
Fukuoka University
151 PUBLICATIONS   **1,673** CITATIONS

SEE PROFILE

(20) Griffiths, R. B. *Phys. Rev.* 1975, *B12*, 345.
(21) Griffiths, R. B.; Wheeler, J. C. *Phys. Rev.* 1970, *A2*, 1047.
(22) Bartis, J. T.; Hall, C. K. *Physica* 1974, *78*, 1. Wheeler, J. C.; Anderson, G. R. *J. Chem. Phys.* 1968, *73*, 5778. Walker, J. S.; Vause, C. A. *J. Chem. Phys.* 1983, *79*, 2660.

(23) Lang, J. C., Jr.; Widom, B. *Physica* 1975, *81A*, 190. Fisher, M. E.; Sarbach, S. *Phys. Rev. Lett.* 1978, *41*, 1127.
(24) Corrales, L. R.; Wheeler, J. C. *J. Chem. Phys.* 1989, *91*, 7097. Also Corrales, L. R. Ph.D. Dissertation, University of California, San Diego, unpublished.

NMR Study on Dynamics of Water Molecules in Concentrated Aqueous Zinc(II) Bromide Solutions at Various Temperatures
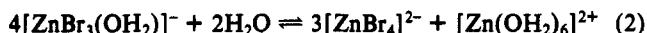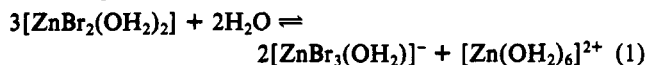
Toshiyuki Takamuku,[†] Toshimi Hirano, Toshio Yamaguchi,* and Hisanobu Wakita

Department of Chemistry, Faculty of Science, Fukuoka University, Nanakuma, Jonan-ku, Fukuoka 814-01, Japan (Received: July 24, 1992)

The proton spin–lattice relaxation time, the deuteron quadrupole relaxation time, and the proton self-diffusion coefficient in aqueous zinc(II) bromide solutions with the water to solute molar ratios of 5 and 10 have been determined by the NMR method as a function of temperature. The proton relaxation time has been divided into the intermolecular and intramolecular contributions of the proton dipole–dipole interaction by using the proton self-diffusion data to derive the translational and rotational correlation times with temperature. The rotational correlation time has also been calculated from the deuteron quadrupole relaxation time. On the basis of the temperature dependence of the translational and rotational correlation times, the dynamics of water molecules and the equilibrium shift of chemical species in the aqueous zinc(II) bromide solutions with temperature are discussed.

Introduction

Aqueous zinc(II) halide solutions have so far been investigated for complex formation[1-10] and chemical structures.[11-20] Recently, interest has been focused on the structure and properties of aqueous zinc(II) halide solutions at nonambient conditions like supercooled and glassy states and high temperatures and pressures. The compositions of solute species in glassy aqueous zinc(II) halide solutions at liquid nitrogen temperature have been revealed from Raman spectroscopic measurements by Kanno and Hiraishi[21] and of a 3.72 *m* aqueous zinc(II) bromide solution at temperatures up to 573 K and pressures up to 9 MPa by Yang et al.[22] We have made X-ray diffraction and X-ray absorption fine structure measurements[23-26] on aqueous zinc(II) halide solutions over a wide temperature range (77–413 K) and determined the structures of average complex species in the solutions. Both X-ray diffraction and Raman scattering data on aqueous zinc(II) bromide solutions have suggested that the following equilibrium shifts take place with temperature:

$$3[ZnBr_2(OH_2)_2] + 2H_2O \rightleftharpoons$$
$$2[ZnBr_3(OH_2)]^- + [Zn(OH_2)_6]^{2+} \quad (1)$$

$$4[ZnBr_3(OH_2)]^- + 2H_2O \rightleftharpoons 3[ZnBr_4]^{2-} + [Zn(OH_2)_6]^{2+} \quad (2)$$

The equilibria (1) and (2) shift to the right-hand side with decreasing temperature and in the opposite direction with increasing temperature. The equilibrium shifts have been discussed in terms of static microscopic structures of the solutions; when the temperature is lowered, in particular, below the melting point of water, the hydrogen bonds are reinforced in the solutions. Correspondingly, water molecules expelled from the dibromo- and tribromozinc(II) complexes will be stabilized in the strengthened hydrogen-bond networks; bromide ions will bind easily to zinc(II) ion. Since water molecules play an important role in the hydrogen-bonded network, it is of great interest to investigate the dynamic behavior of water molecules in aqueous zinc(II) halide solutions over a wide range of temperature to discuss the equilibrium shifts from dynamic properties of the solutions.

TABLE I: Composition of the Sample Solutions (mol kg⁻¹)

solution	Zn^{2+}	Br^-	$[H_2O]/$ $[ZnBr_2]$	$[D_2O]/$ $[ZnBr_2]$
A	10.64	21.28	5.22	
B	5.493	10.99	10.1	
C	9.480	18.96		5.26
D	4.867	9.734		10.3

The motions of water molecules in liquid water and in aqueous electrolyte solutions have often been investigated in terms of the spin–lattice relaxation time and the correlation time from NMR relaxation measurements on ^1H, ^2H (D), and ^{17}O nuclei of the water molecule.[27-36] The self-diffusion coefficients of water molecules have also been measured by the NMR spin–echo method for electrolyte solutions.[37]

For concentrated aqueous zinc(II) chloride solutions, Nakamura et al.[38] measured the proton self-diffusion coefficient and spin-lattice relaxation time as a function of solute concentration and temperature and have concluded that the translational motion of water molecules in the solutions is retarded more rapidly than the rotational motion with decreasing water content.

In the present study we have measured the proton self-diffusion coefficient and the proton and deuteron spin-lattice relaxation times in aqueous zinc(II) bromide solutions in H_2O and D_2O, with the water to solute molar ratios of 5 and 10 as a function of temperature. The proton spin-lattice relaxation time measured has been divided into the intermolecular and intramolecular contributions of the dipole–dipole interaction, from which the translational and rotational correlation times of the water molecule have been estimated as a function of temperature. The rotational correlation of the water molecule has also been derived directly from the deuteron spin–lattice relaxation time. Finally, the translational and rotational motions of water molecules and the equilibrium shifts (1) and (2) with temperature will be discussed in terms of the translational and rotational correlation times obtained.

Experimental Section

Preparation of Sample Solutions. Zinc(II) bromide (Wako Pure Chemicals, 99.9%) was used without further purification and

---

*To whom correspondence should be addressed.
†On leave from Aqua Laboratory, Research and Development Division, TOTO Ltd., Nakashima, Kokurakita-ku, Kitakyushu 802, Japan.
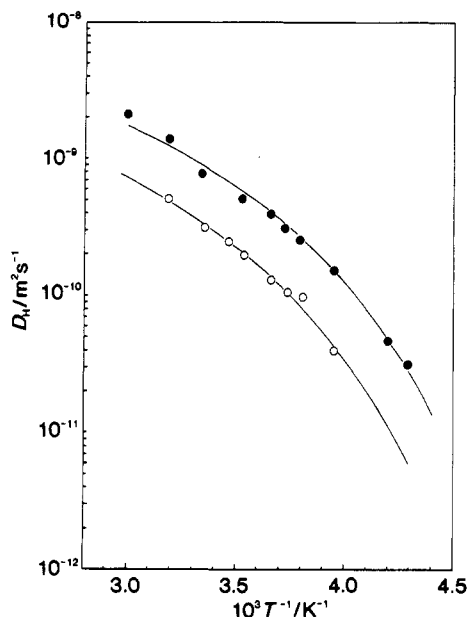
Figure 1. ¹H self-diffusion coefficient D_H for solution A (opened circle) and solution B (filled circle) against the reciprocal temperature. The solid line corresponds to a VTF-type theoretical curve. Fitted values of D_{H0} and B are given in Table II.

dissolved in distilled water to reach the water-to-solute molar ratios (R) of 5 and 10. The corresponding heavy water solutions were also prepared by dissolving zinc(II) bromide in heavy water (ISOTEC Inc., 99.9%).

The concentrations of zinc(II) ions in the sample solutions were determined by titration of an EDTA standard solution, using Eriochrome Black T as an indicator. The compositions of the sample solutions are given in Table I.

NMR Measurements. Prior to NMR measurements oxygen gas dissolved in the sample solution was removed by bubbling pure nitrogen gas for 15 min. The sample solution was sealed in a double-walled glass tube, i.e., a usual NMR tube of 10-mm diameter with an oval microcell inside.

NMR measurements were carried out by using a 200-MHz spectrometer (JEOL JNM-FX200). The temperature of sample solution was measured with a copper–constantan thermocouple and controlled within ±0.3 °C by hot air and/or a dry nitrogen stream from liquid nitrogen.

The proton self-diffusion coefficient for solutions A and B was measured in a temperature range from 233 to 333 K by the pulsed gradient method.[39] Two field gradient pulses g were applied to the sample solution at $t = t_1$ ($0 < t_1 < \tau$) and $t = t_1 + \Delta$. The decay of the echo amplitude A is given by

$$\ln [A(g,2\tau)/A(0,2\tau)] = -\gamma_H^2 \delta^2 g^2 (\Delta - \delta/3) D_H \qquad (3)$$

where τ represents the time between the 90° and the 180° pulses applied, γ_H is the gyromagnetic ratio of a proton, D_H is the proton self-diffusion coefficient, δ is the duration of the gradient pulses, and Δ is the time between the two gradient pulses. The g value was calibrated by using a known D_H value for pure water. The values of D_H were determined by varying Δ under the condition of $\Delta = \tau$ at constants g and δ. The current of the gradient coil was supplied with a pulse gradient generator (JEOL NM PL-200). The magnitude of g ranged from 13.52 to 63.5 G cm⁻¹ and that of δ from 1.0 to 9 ms, with Δ of 100.5 ms.

The proton and deuteron spin-lattice relaxation times, $T_{1,H}$ and $T_{1,D}$, for solutions A, B, C, and D, were measured over a temperature range from 203 to 333 K by the inversion recovery method with the 180°–τ–90° pulse sequence.

Results and Discussion

Proton Self-Diffusion Coefficient. The proton self-diffusion coefficient, D_H, measured for solutions A and B was plotted as a function of the reciprocal temperature in Figure 1. As is seen

TABLE II: Optimized Parameter Values of VTF Fitting for the Proton Self-Diffusion Coefficient of Solutions A and B

solution	$10^8 D_{H0}/\text{m}^2\,\text{s}^{-1}$	$B/\text{kJ mol}^{-1}$
A	1.11	3.55
B	1.76	3.04

TABLE III: Smoothed Values of the Proton Self-Diffusion Coefficient, the Proton Spin–Lattice Relaxation Rate, the Intermolecular and Intramolecular Contributions, and the Deuteron Spin–Lattice Relaxation Rate for Solutions A and C ($R = 5$) in the Temperature Range 243–333 K

T/K	$10^9 D_H/\text{m}^2\,\text{s}^{-1}$	$R_{1,H}/\text{s}^{-1}$	$R_{1,H}^{\text{inter}}/\text{s}^{-1}$	$R_{1,H}^{\text{intra}}/\text{s}^{-1}$	$R_{1,D}/\text{s}^{-1}$
333	0.733	0.489	0.274	0.215	2.72
323	0.613	0.606	0.323	0.283	3.47
313	0.495	0.771	0.391	0.380	4.52
303	0.383	1.01	0.490	0.522	6.07
298	0.338	1.15	0.546	0.605	6.97
293	0.289	1.35	0.623	0.722	8.26
283	0.206	1.85	0.821	1.03	11.8
273	0.136	2.64	1.12	1.52	18.2
263	0.0819	3.85	1.58	2.27	30.3
253	0.0433	5.58	2.18	3.40	56.0
243	0.0192	7.69	2.67	5.03	116

TABLE IV: Smoothed Values of the Proton Self-Diffusion Coefficient, the Proton Spin–Lattice Relaxation Rate, the Intermolecular and Intramolecular Contributions, and the Deuteron Spin–Lattice Relaxation Rate for Solutions B and D ($R = 10$) in the Temperature Range 233–333 K

T/K	$10^9 D_H/\text{m}^2\,\text{s}^{-1}$	$R_{1,H}/\text{s}^{-1}$	$R_{1,H}^{\text{inter}}/\text{s}^{-1}$	$R_{1,H}^{\text{intra}}/\text{s}^{-1}$	$R_{1,D}/\text{s}^{-1}$
333	1.72	0.304	0.152	0.152	1.99
323	1.48	0.362	0.176	0.185	2.37
313	1.23	0.444	0.210	0.233	2.96
303	0.987	0.563	0.259	0.304	3.90
298	0.887	0.632	0.286	0.346	4.45
293	0.776	0.730	0.324	0.406	5.24
283	0.580	0.990	0.422	0.568	7.36
273	0.408	1.41	0.577	0.836	10.8
263	0.264	2.12	0.833	1.29	16.8
253	0.153	3.29	1.27	2.02	27.6
243	0.0761	5.16	2.03	3.13	49.8
233	0.0287	7.91	3.07	4.84	108

in Figure 1, the self-diffusion coefficients for both solutions decrease exponentially with lowering the temperature. Since the amount of "excess protons" is low in the present system, the proton transfer is expected to be made by molecular diffusion.[40] Thus, Figure 1 shows that the translational motion of water molecules in the present solutions is gradually hindered with lowering the temperature. In solution B, which includes a larger amount of water molecules than solution A, the diffusion coefficient is larger than that for solution A (Figure 1).

As is apparent in Figure 1 the T^{-1} dependence of log D_H is not of Arrhenius type. Lang and Lüdemann[32] have suggested that the dynamic properties of supercooled solutions can be well represented by a modified Arrhenius equation, i.e., Vogel–Tammann–Fulcher (VTF) equation

$$D_H = D_{H0} \exp[-B/(T - T_0)] \qquad (4)$$

This empirical equation describes the slowing down of the diffusion coefficient in aqueous solution approaching its glass transition point T_0. The self-diffusion coefficients measured at the various temperatures in the present study were fitted by using the VTF equation with $T_0 = 176$ K as the glass transition temperature, which was determined with DSC measurement for solution A in a previous study.[26] The parameters optimized for both solutions are listed in Table II. As seen in Figure 1, theoretical curves have reproduced satisfactorily the measured values of the diffusion coefficient. The smoothed D_H values for solutions A and B at the various temperatures are given in Tables III and IV. The smoothed values at 298 K, D_H = 0.338 × 10⁻⁹ and 0.887 × 10⁻⁹ m² s⁻¹ for solutions A and B, respectively, are comparable with those of 0.243 × 10⁻⁹ and 0.634 × 10⁻⁹ m² s⁻¹ for aqueous zinc(II)
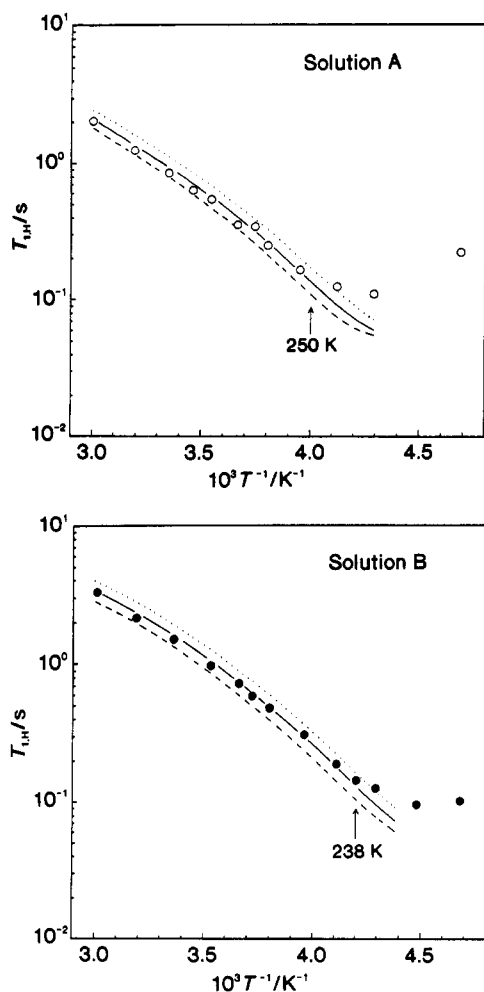
Figure 2. Temperature dependence of the proton relaxation times $T_{1,H}$. The observed values are plotted for solution A (opened circle) and solution B (filled circle). The calculated $T_{1,H}$ values with $\tau_{D,ice}$, $\tau_{D,liq}$, and $\tau_{D,gas}$ are drawn by the broken, solid, and dotted lines, respectively.

chloride solutions with $[H_2O]/[ZnCl_2]$ molar ratios of 4.1 and 7.4, respectively.[38]

Proton Spin–Lattice Relaxation Rate. Figure 2 shows the temperature dependence of the proton spin-lattice relaxation time $T_{1,H}$ for solutions A and B. A minimum of the relaxation time appears around 230 and 219 K for solutions A and B, respectively. The temperature-dependent behaviors of $T_{1,H}$ for both solutions are similar to that found for an aqueous zinc(II) chloride solution with $[H_2O]/[ZnCl_2] = 4.1$,[38] in which a minimum of the relaxation time was observed around 233 K.

In the present work, the proton spin-lattice relaxation rate, $R_{1,H}$ ($=1/T_{1,H}$), has been divided into the contributions from the intermolecular and intramolecular dipole–dipole interactions in the following procedure. In the present aqueous zinc(II) bromide solutions the compositions of the predominant zinc(II) bromo complexes, $[ZnBr_n(OH_2)_{4-n}]^{(2-n)+}$ ($n = 2$, 3, and 4), change with temperature;[25,26] hence, the number of interactions between the water molecule and zinc(II) ion is not constant over the temperature range investigated. Therefore, it is difficult to analyze the relaxation rate with a simple model such as the two-site approximation that has been adopted to analyze the proton relaxation in aqueous lithium chloride solutions by Lang and Prielmeier.[35] In highly concentrated aqueous solutions, as in the present case, all water molecules probably bind to the ions; the spin-lattice relaxation rate in water is governed mainly by the intermolecular and intramolecular ^1H–^1H dipole–dipole interactions in the temperature range; i.e., the relaxation rate can be expressed as the sum of the intermolecular $R_{1,H}^{inter}$ and the intramolecular $R_{1,H}^{intra}$ parts

$$R_{1,H} = R_{1,H}^{inter} + R_{1,H}^{intra} \tag{5}$$

TABLE V: Estimated Values of the Translational and the Rotational Correlation Times for Solutions A and C ($R = 5$) in the Temperature Range 243–333 K

T/K	τ_{inter}/ps	τ_{intra}/ps	$\tau_{D,ice}{}^a$/ps	$\tau_{D,liq}{}^a$/ps	$\tau_{D,gas}{}^a$/ps
333	51.9	3.09	4.00	2.83	1.93
323	62.1	4.07	5.10	3.61	2.46
313	76.9	5.46	6.64	4.71	3.20
303	99.4	7.51	8.91	6.32	4.30
298	113	8.70	10.2	7.25	4.93
293	132	10.4	12.1	8.59	5.85
283	185	14.8	17.4	12.3	8.38
273	280	21.8	26.7	18.9	12.9
263	465	32.7	44.5	31.6	21.5
253	880	48.9	82.2	58.3	39.7
243	1990	72.3	170	120	81.9

[a] The values were calculated by using the deuteron quadrupole coupling constants and asymmetry parameters for ice, liquid, and gas phases, respectively.

TABLE VI: Estimated Values of the Translational and the Rotational Correlation Times for Solutions B and D ($R = 10$) in the Temperature Range 233–333 K

T/K	τ_{inter}/ps	τ_{intra}/ps	$\tau_{D,ice}{}^a$/ps	$\tau_{D,liq}{}^a$/ps	$\tau_{D,gas}{}^d$/ps
333	22.1	2.18	2.92	2.07	1.41
323	25.8	2.67	3.48	2.46	1.68
313	31.0	3.35	4.35	3.08	2.10
303	38.6	4.38	5.72	4.06	2.76
298	42.9	4.97	6.53	4.63	3.15
293	49.1	5.83	7.69	5.45	3.71
283	65.6	8.17	10.8	7.66	5.21
273	93.5	12.0	15.9	11.3	7.67
263	145	18.5	24.6	17.4	11.9
253	249	29.0	40.6	28.8	19.6
243	500	45.0	73.1	51.8	35.3
233	1330	69.5	158	112	76.4

[a] The values were calculated by using the deuteron quadrupole coupling constants and asymmetry parameters for ice, liquid, and gas phases, respectively.

The spin–rotation contribution is negligible in the temperature range studied.[30]

The intermolecular contribution, $R_{1,H}^{inter}$, will be to a large extent modulated by translational motion of water molecule[32] and is expressed as

$$R_{1,H}^{inter} = (6\pi/5)(\gamma_H^2 \hbar(\mu_0/4\pi))^2 (N_H/2D_H d_{HH}) F(\omega_H \tau_{inter}) \tag{6}$$

with

$$F(\omega_H \tau_{inter}) = 2g(\omega_H \tau_{inter}) + 8g(2\omega_H \tau_{inter}) \tag{7}$$

$$g(\omega_H \tau_{inter}) = [(3/2)u^2 + (15/2)u + 12] \times [(1/8)u^6 + u^5 + 4u^4 + (27/2)u^3 + (81/2)u^2 + 81u + 81]^{-1} \tag{8}$$

$$u^2 = 2\omega_H \tau_{inter} \tag{9}$$

Here $\hbar$ is the Planck constant divided by 2π, μ_0 is magnetic permeability under vacuum, N_H is the number density of proton, and ω_H is the Larmor frequency under the experimental conditions. τ_{inter} is the correlation time for the intermolecular dipole–dipole interaction, corresponding to the translational correlation time of water molecule.

The translational correlation time τ_{inter} is related to the experimentally determined self-diffusion coefficient D_H with

$$\tau_{inter} = d_{HH}^2/2D_H \tag{10}$$

where d_{HH} is the distance of closest approach between two protons of intermolecular water molecules. In the present study a value of 276 pm was used for d_{HH}, which has been estimated from the diameter of the water molecule.[38] The translational correlation time for solutions A and B has been estimated as a function of temperature by using eq 10 with the self-diffusion coefficients listed
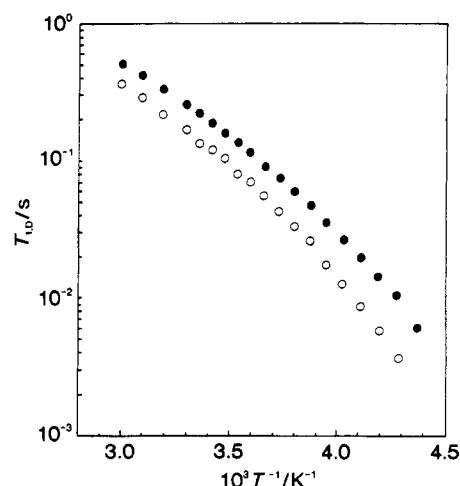
Figure 3. Temperature dependence of the deuteron relaxation times $T_{1,D}$ for solutions C (opened circle) and B (filled circle).

in Tables III and IV. The final results are given in Tables V and VI.

The intramolecular relaxation rate, $R_{1,H}^{intra}$, which is contributed from the rotational motion of water molecules,[32] is given by

$$R_{1,H}^{intra} = (3/20)(\gamma_H^2 \hbar(\mu_0/4\pi))^2 \langle r_{HH}^{-3} \rangle^2 F(\omega_H \tau_{intra}) \quad (11)$$

with

$$F(\omega_H \tau_{intra}) = [2\tau_{intra}/(1 + \omega_H^2 \tau_{intra}^2) + 8\tau_{intra}/(1 + 4\omega_H^2 \tau_{intra}^2)] \quad (12)$$

where $\langle r_{HH}^{-3} \rangle$ is the average distance between the protons within a water molecule. τ_{intra} is the correlation time for the intramolecular dipolar interaction, corresponding to the rotational correlation time of the water molecule.

In the present study, first, the experimentally obtained values of the spin-lattice relaxation time were fitted to a fourth-order equation as a function of temperature by a least-squares method. Second, the intramolecular contribution, $R_{1,H}^{intra}$, was derived by subtracting the intermolecular contribution, $R_{1,H}^{inter}$, calculated by using eqs 6–10 from the smoothed R_H value in eq 5. Finally, the correlation time τ_{intra} in the fast motion regime, $\omega_H \tau_r \ll 1$, was calculated by using the reduced eq 13 with the distance $r_{HH} =$

$$R_{1,H}^{intra} = (3/2)(\gamma_H^2 \hbar(\mu_0/4\pi))^2 \langle r_{HH}^{-3} \rangle^2 \tau_{intra} \quad (13)$$

151.9 pm derived from the geometry of a water molecule ($r_{OH} = 96$ pm, H–O–H angle $= 104.5°$).

For both aqueous solutions, the smoothed values of $R_{1,H}$, $R_{1,H}^{inter}$, and $R_{1,H}^{intra}$ are summarized in Tables III and IV. The translational and rotational correlation times, τ_{inter} and τ_{intra}, respectively, estimated in the above procedures are listed in Tables V and VI.

Deuteron Quadrupolar Relaxation. In the previous section, the values of $R_{1,H}^{intra}$ have been calculated by subtraction of the estimated $R_{1,H}^{inter}$ values from the experimental $R_{1,H}$ values. Therefore, the uncertainties in τ_{intra} depend on the estimation of $R_{1,H}^{inter}$. The rotational correlation time can also be evaluated directly from the deuteron spin-lattice relaxation time, $T_{1,D}$, to which the quadrupole interaction due to the rotational motion of water molecules contributes. The $T_{1,D}$ values for heavy water solutions C and D have been plotted in Figure 3; the relaxation time decreases exponentially as a function of reciprocal temperature. A minimum of the relaxation time was not observed for both solutions in the present temperature range.

The relaxation of the deuteron is dominated mainly by a coupling of the electric quadrupole moment eQ of the nucleus to the electronic field gradient eq at the nucleus. The relation between the spin–lattice relaxation rate, $R_{1,D}$, and the rotational correlation time, τ_D, is expressed as[32]

$$R_{1,D} = (3/80)(e^2qQ/\hbar)^2(1 + \eta^2/3)F(\omega_D \tau_D) \quad (14)$$

with $F(\omega_D \tau_D)$ given by eq 12. Here, $e^2qQ/\hbar$ and η are the

quadrupole coupling constant and the asymmetry parameter, respectively. Under the condition of fast motion regime, $\omega_D \tau_D \ll 1$, eq 14 is reduced to

$$R_{1,D} = (3/8)(e^2qQ/\hbar)^2(1 + \eta^2/3)\tau_D \quad (15)$$

The value of $e^2qQ/\hbar$ for the liquid phase cannot be measured directly, while those for ice (214 kHz) and for gas (307.9 kHz) have been determined experimentally.[27] Struis et al.[29] estimated the values of $e^2qQ/\hbar$ for pure water and coordinated water within the first coordination shell of the Mg^{2+} ion in the temperature region 263–326 K from the relaxation rates of D and ^{17}O nuclei. The values obtained are 254 kHz for pure water and 213 kHz for coordinated water at 298 K; the latter is very similar to that for the ice phase. They have suggested that these values hardly change with temperature and concentration of magnesium chloride. In this study, the rotational correlation times for three phases of ice (214 kHz), liquid (254 kHz), and gas (307.9 kHz) were calculated for a comparison. The asymmetry parameters η for ice, liquid, and gas phases used were 0.12,[27] 0.135,[29] and 0.135,[27] respectively. However, the asymmetry parameter hardly affects the spin–lattice relaxation rate of the deuteron because the value of $\eta^2/3$ is so small, $\eta^2/3 < 0.006$.

The deuteron spin-lattice relaxation rates, $R_{1,D}$, smoothed with the fourth-order polynomial, are listed in Tables III and IV for solutions C and D, respectively. The rotational correlation time has been derived from the smoothed $R_{1,D}$ value by using eq 15, as a function of temperature in the fast motion regime ($\omega_D \tau_D \ll 1$). The values of the rotational correlation times, $\tau_{D,ice}$, $\tau_{D,liq}$, and $\tau_{D,gas}$, calculated by using the constants for the ice, liquid, and gas phases, respectively, are summarized in Tables V and VI.

Translational and Rotational Correlation Times. Tables V and VI show that the translational (τ_{inter}) and the rotational (τ_{intra}) correlation times at 298 K are 113 and 8.70 ps for solution A and 42.9 and 4.97 ps for solution B, respectively. The values are comparable with those obtained for aqueous zinc(II) chloride solutions; $\tau_{inter} = 88.8$ ps and $\tau_{intra} = 12.3$ ps for the solution of $R = 4.1$, 34.0 and 7.26 ps for the solution of $R = 7.4$.[38] For solutions A and B, the values of the rotational correlation time, τ_{intra}, fall between $\tau_{D,ice}$ and $\tau_{D,gas}$ in the temperature range investigated. Furthermore, the values of τ_{intra} are in good agreement with those of $\tau_{D,liq}$.

In order to further confirm the feasibility of the present treatment, the proton relaxation rates $R_{1,H}$ were reversely calculated in the following way and compared with the observed ones. First, the values of $R_{1,H}^{intra}$ for ice, liquid, and gas were calculated by using eqs 11 and 12 with $\tau_D = \tau_{intra}$. Next, $R_{1,H}^{inter}$ was estimated by using eqs 6–10 with the experimental D_H. Finally, $R_{1,H}$ was obtained by using eq 5 with the $R_{1,H}^{inter}$ and $R_{1,H}^{intra}$ derived above. The simulated curves are drawn in Figure 2. Apparently, the observed $T_{1,H}$ values fall between those calculated using $\tau_{D,ice}$ and $\tau_{D,gas}$ above ~250 and 238 K for solutions A and B, respectively, and are best reproduced when $\tau_{D,liq}$ was used. These results demonstrate that the rotational correlation time has been reasonably estimated by the present model of the proton magnetic relaxation, eqs 5–13, over the above-mentioned temperatures for both solutions. Below these temperatures, however, other processes will contribute to the relaxation. Therefore, we will discuss the translational and rotational motions of water molecules in terms of τ_{inter} and $\tau_{D,liq}$ above ~250 and 238 K for solutions A and B, respectively.

The temperature-dependent translational (τ_{inter}) and rotational ($\tau_{D,liq}$) correlation times are plotted in Figure 4. The correlation times for the solutions with $R = 5$ and 10 increase with decreasing temperature; both curves are nearly parallel. Water molecules in the solutions probably behave in a similar manner as the temperature decreases. Furthermore, τ_{intra} and $\tau_{D,liq}$ for the solution with $R = 10$ are smaller than those for the solution with $R = 5$ within the present temperature range, suggesting that water molecules move more freely in the former solution than in the latter solution. As seen in Figure 4, differences in the translational correlation time between both solutions are larger than those in the rotational correlational times. This finding suggests that the
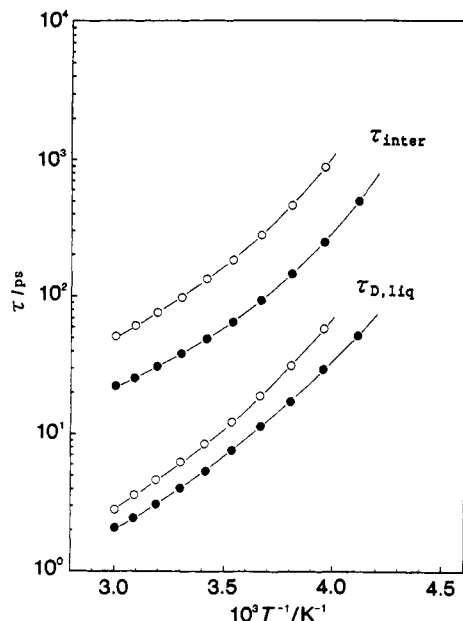
Figure 4. Correlation times, τ_{inter}, and $\tau_{D,liq}$ for solutions with $R = 5$ (opened circle) and 10 (filled circle) against reciprocal temperature.
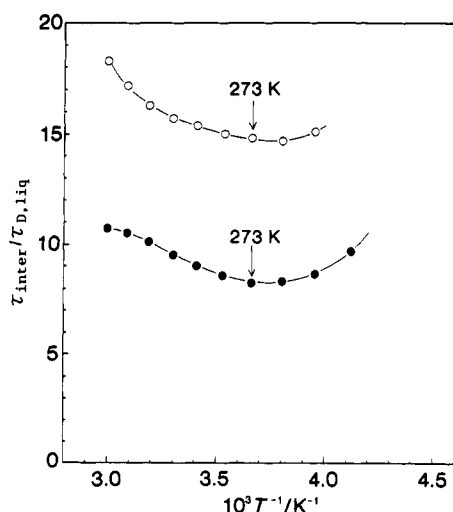

Figure 5. Temperature dependence of the ratio $\tau_{inter}/\tau_{D,liq}$ for solutions with $R = 5$ (opened circle) and 10 (filled circle).

rotational motion of water molecules has less concentration dependence than the translational motion.

In order to more clearly discuss the temperature dependence of the individual correlation times, the $\tau_{inter}/\tau_{D,liq}$ ratios are plotted in Figure 5 against the reciprocal temperature. In the temperature range studied the $\tau_{inter}/\tau_{D,liq}$ ratio is larger for the solution with $R = 5$ than for the solution with $R = 10$, indicating again that the translational motion of water in the former solution is more restricted than in the latter solution. A similar concentration dependence of the translational motion of water molecules has also been found for aqueous zinc(II) chloride solutions with various $[H_2O]/[ZnCl_2]$ molar ratio from 2 to 7.4 at ambient temperature.[38]

For both solutions the $\tau_{inter}/\tau_{D,liq}$ ratio decreases with lowering the temperature to around 273 K but increases with temperature below 273 K. This behavior suggests that the motion of water molecules in the aqueous zinc(II) bromide solutions do not slow down monotonously with lowering the temperature. It should be noted that the equilibrium shifts (1) and (2) take place with decreasing temperature,[25,26] affecting the dynamics behavior of water molecules.

Now we discuss the behavior of the $\tau_{inter}/\tau_{D,liq}$ ratio on the basis of the equilibrium shifts with temperature. At high and ambient temperatures, the dibromo and tribromo complexes are preferentially formed in the aqueous zinc(II) bromide solutions.[25] This

is probably because water molecules, 2.5 and 5 times more than bromide ions in the two solutions, frequently occupy the coordination sites of a zinc(II) ion. In other words, the translational motion of water molecules is restricted mainly through binding to zinc(II) ion and thus will be not sensitive to temperature. Thus, the translational correlation time τ_{inter} increases more slowly than the rotational correlation time $\tau_{D,liq}$ with decreasing temperature. As a result, the $\tau_{inter}/\tau_{D,liq}$ ratio decreases with lowering the temperature down to about 273 K.

With further lowering of temperature, in particular, below the melting point of water, on the contrary, the formation of the tetrabromozinc(II) complex is favored in the aqueous zinc(II) bromide solutions.[26] This means that water molecules within the dibromo- and tribromozinc(II) complexes are expelled from the first coordination shell and are stabilized in strengthened hydrogen-bonded networks. Thus, the translational motion of the water molecules in the supercooled solutions will be restricted more strongly than in the solutions at ambient and higher temperatures. Therefore, the translational correlation time τ_{inter} will increase more sharply than the rotational correlation time $\tau_{D,liq}$ below the melting point of water, leading to the increase in the $\tau_{inter}/\tau_{D,liq}$ ratio with lowering the temperature below about 273 K.

In conclusion, the temperature-dependent motions of water molecules in the aqueous zinc(II) bromide solutions with $R = 5$ and 10 have been demonstrated from measurements of both proton and deuteron spin–lattice relaxation times and the proton self-diffusion coefficients by NMR. In the supercooled solutions the translational motion of water molecules is hindered more quickly than the rotational motion. This conclusion on the dynamic properties of water molecules supports well that the enhancement of hydrogen bonding with lowering the temperature causes the equilibrium shifts (1) and (2) in the aqueous zinc(II) halide solutions.

References and Notes

(1) Bernhard, M. A.; Busnot, F.; Le Querler, J. F. *Bull. Soc. Chim. Fr.* **1972**, 4523.
(2) Shchukarev, S. A.; Lilich, L. S.; Latysheva, V. A. *Zh. Neorg. Khim.* **1956**, *1*, 225.
(3) Ahrland, S.; Rosengren, K. *Acta Chem. Scand.* **1956**, *10*, 727.
(4) Horne, R. A.; Holm, R. H.; Meyers, M. D. *J. Phys. Chem.* **1957**, *61*, 1661.
(5) Connick, R. E.; Paul, A. D. *J. Am. Chem. Soc.* **1958**, *80*, 2069.
(6) Tribalat, S.; Dutheil, C. *Bull. Soc. Chim. Fr.* **1960**, 160.
(7) Short, E. L.; Morris, D. F. C. *J. Inorg. Nucl. Chem.* **1961**, *18*, 192.
(8) Dyrssen, D.; De Jesus Tavares, M. *Acta Chem. Scand.* **1966**, *20*, 2050.
(9) Gerding, P. *Acta Chem. Scand.* **1969**, *23*, 1695.
(10) Ahrland, S.; Kullberg, L.; Portanova, R. *Acta Chem. Scand.* **1978**, *A32*, 251.
(11) Irish, D. E. In *Ionic Interactions*; Petrucci, S., Ed.; Academic Press: New York, 1971; Vol. II, pp 239–246.
(12) Delwaulle, M. L. *C. R. Acad. Sci.* **1955**, *240*, 2132; *Bull. Soc. Chim. Fr.* **1955**, 1294.
(13) Irish, D. E.; McCarroll, B.; Young, T. F. *J. Chem. Phys.* **1963**, *39*, 3426.
(14) Morris, D. F. C.; Short, E. L.; Slater, K. *Electrochim. Acta* **1963**, *8*, 289.
(15) Gilbert, B. *Bull. Soc. Chim. Belges.* **1967**, *76*, 493.
(16) Fontana, M. P.; Maisano, G.; Migliardo, P.; Wanderlingh, F. *J. Chem. Phys.* **1978**, *69*, 676.
(17) (a) Wertz, D. L.; Bell, J. R. *J. Inorg. Nucl. Chem.* **1973**, *35*, 137; (b) *Ibid.* **1973**, *35*, 861.
(18) Goggin, P. L.; Johansson, G.; Maeda, M.; Wakita, H. *Acta Chem. Scand.* **1984**, *A38*, 625.
(19) Wakita, H.; Johansson, G.; Sandström, M.; Goggin, P. L.; Ohtaki, H. *J. Solution Chem.* **1991**, *20*, 643.
(20) Yamaguchi, T.; Hayashi, S.; Ohtaki, H. *J. Phys. Chem.* **1989**, *93*, 2620.
(21) Kanno, H.; Hiraishi, J. *J. Raman Spectrosc.* **1980**, *9*, 85.
(22) Yang, M. M.; Crerar, D. A.; Irish, D. E. *J. Solution Chem.* **1988**, *17*, 751.
(23) Yamaguchi, T.; Kamihata, K.; Wakita, H.; Nomura, M. *Photon Factory Activity Report.* National Laboratory for High Energy Physics,

KEK-PF, Tsukuba, 1988; Vol. 6, p 45.
   (24) Takamuku, T.; Yamaguchi, T.; Wakita, H. J. Phys. Chem. 1991, 95, 10098.
   (25) Takamuku, T.; Ihara, M.; Yamaguchi, T.; Wakita, H. Z. Naturforsch. 1992, 47a, 485.
   (26) Takamuku, T.; Yoshikai, K.; Yamaguchi, T.; Wakita, H. Z. Naturforsch. 1992, 47a, 841.
   (27) Lankhorst, D.; Schriever, J.; Leyte, J. C. Ber. Bunsen-Ges. Phys. Chem. 1982, 86, 215.
   (28) Van der Maarel, J. R. C.; Lankhorst, D.; De Bleijser, J.; Leyte, J. C. J. Phys. Chem. 1986, 90, 1470.
   (29) Struis, R. P. W. J.; De Bleijser, J.; Leyte, J. C. J. Phys. Chem. 1987, 91, 1639.
   (30) Jonas, J.; DeFries, T.; Wilbur, D. J. J. Chem. Phys. 1976, 65, 582.
   (31) Lang, E. W.; Bradl, S.; Fink, W.; Radkowitsch, H.; Girlich, D. J. Phys.: Condens. Matter. 1990, 2, 195.

   (32) Lang, E. W.; Lüdemann, H.-D. In NMR Basic Principles and Progress; Springer-Verlag: Berlin, 1990; Vol. 24, pp 130–187.
   (33) (a) Shimizu, A.; Taniguchi, Y. Bull. Chem. Soc. Jpn. 1990, 63, 1572. (b) Ibid. 1990, 63, 3255.
   (34) Harmon, J. F.; Sutter, E. J. J. Phys. Chem. 1978, 82, 1938.
   (35) Lang, E. W.; Prielmeier, F. X. Ber. Bunsen-Ges. Phys. Chem. 1988, 92, 717.
   (36) Hasebe, T.; Tamamushi, R.; Tanaka, K. J. Chem. Soc., Faraday Trans. 1992, 88, 205.
   (37) Prielmeier, F. X.; Lang, E. W.; Speedy, R. J.; Lüdemann, H.-D. Ber. Bunsen-Ges. Phys. Chem. 1988, 92, 1111.
   (38) Nakamura, Y.; Shimokawa, S.; Futamata, K.; Shimoji, M. J. Chem. Phys. 1982, 77, 3258.
   (39) Stejskal, E. O.; Tanner, J. E. J. Chem. Phys. 1965, 42, 288.
   (40) Girard, C.; Braunstein, J.; Bacarella, A. L.; Benjamin, B. M.; Brown, L. L. J. Chem. Phys. 1977, 67, 1555.

Rheology of Ternary Microemulsions

Chih-Ming Chen and Gregory G. Warr*

School of Chemistry, The University of Sydney, Sydney, NSW, 2006, Australia (Received: January 22, 1992; In Final Form: June 16, 1992)

The flow of ternary microemulsions composed of didodecyldimethylammonium bromide, dodecane, and water under shear has been investigated in both Couette and capillary viscometers. At all compositions studied the liquids were found to be Newtonian up to very high shear rates ($\sim$3000 s^{-1}), although some indirect evidence for elasticity was inferred from capillary viscometry. The dependence of viscosity on composition is discussed and interpreted in terms of the structure of the microemulsion in both bicontinuous and water-in-oil domains.

Introduction

There have been a number of studies detailing the properties of three component microemulsions formed by double-chained quaternary ammonium surfactants with oil and water.[1-3] The most common among these are systems comprising didodecyldimethylammonium bromide (DDAB), water, and a C_6-C_{12} alkane. DDAB is essentially insoluble in both alkanes and water, which makes it attractive as a model surfactant as an inventory of the total area of the alkane/water interface in the microemulsion may easily be kept.

A partial isotropic phase diagram of the DDAB/dodecane/water system, showing the single-phase microemulsion region, is given in Figure 1.[4] Throughout most of the single-phase region, these microemulsions are bicontinuous, as inferred from conductivity,[1] diffusion coefficients,[5] and small-angle scattering.[6,7] However at high water content they undergo a reverse percolation and a structural transformation into water droplets in oil. The boundary between discrete and continuous regions of the microemulsion is indicated by the dashed line in Figure 1.

We are interested in the rheology of such liquids for a number of reasons. Primarily we wish to study the relationship between structure and flow behavior. Three component DDAB microemulsions are ideal models for this study as their structure has been thoroughly examined using a number of techniques, as mentioned above. Importantly the structures formed depend on DDAB/oil/water composition, allowing a variety of equilibrium structures to be investigated within the framework of the same chemical system. It is known from previous work with solutions of cylindrical micelles[8,9] that viscoelastic effects may arise, and the existence of transient bicontinuous networks has been postulated. Bicontinuous microemulsions might well be expected to display similar behavior.

Previous studies of the rheology of microemulsions are scarce. Those that do exist have concentrated on droplet structures, either oil-in-water[10] or water-in-oil dispersions,[11] with little attention to the shear rate dependence. Systematic study of the rheology of

bicontinuous microemulsions has been hampered by a lack of knowledge about the equilibrium structure of the liquid, so that even thorough rheological examination must be analyzed by a more or less arbitrary parametrization.[12] Rheology is not the way to investigate structure. Rather it is the contrary, and a useful interpretation of rheological measurements requires some knowledge of the equilibrium structure so that the perturbative effect of shear may be ascertained. This is why the DDAB/dodecane/water system is ideal for such a purpose.

Application of a shear field to a complex liquid such as a microemulsion holds the promise of a technique for determining the dynamics of reorganization of these systems. About this more is said in connection with the results. In our interpretation of the rheology of these model microemulsions we will need to make reference to what is known about their equilibrium structure and properties. Previous results and the models used for their interpretation are discussed in the following section, after which we return to the immediate issue of their flow behavior.

Structure and Properties of DDAB/Alkane/Water Microemulsions. The microemulsion phase, L_2, delineated by the phase boundary shown in Figure 1, is a single-phase region within which surfactant, dodecane, and water mix to form a clear, thermodynamically stable, isotropic liquid. Alkanes and water are immiscible, and an important feature of this system is that the surfactant DDAB has negligible solubility in either dodecane or water. This is atypical of microemulsions, in which the surfactant may be quite water soluble, and which often include cosurfactants with high oil and/or water solubilities. DDAB prefers insolubility in the case of dodecane and forms a lamellar liquid crystal or vesicular dispersion in water at concentrations above 1×10^{-4} M. In the microemulsion the surfactant can therefore safely be said to all reside at, and indeed stabilize, the internal interface which is formed between the immiscible liquids.

Along the low water phase boundary the microemulsions are all electrically conducting, which indicates that water is a continuous phase in the liquid. As water is added to one of these microemulsions the conductivity decreases, eventually dropping by 3 orders of magnitude to become nonconducting.[1] Nuclear

---